J Paleolimnol (2011) 46:351–367
DOI 10.1007/s10933-010-9443-3

ORIGINAL PAPER

Climate and human impact on a meromictic lake during the last 6,000 years (Montcortès Lake, Central Pyrenees, Spain)

Juan Pablo Corella · Ana Moreno · Mario Morellón · Valentí Rull · Santiago Giralt · María Teresa Rico · Ana Pérez-Sanz · Blas Lorenzo Valero-Garcés

Received: 11 September 2009 / Accepted: 26 April 2010 / Published online: 14 May 2010

Abstract Sedimentological, mineralogical and compositional analyses performed on short gravity cores and long Kullenberg cores from meromictic Montcortès Lake (Pre-Pyrenean Range, NE Spain) reveal large depositional changes during the last 6,000 cal years. The limnological characteristics of this karstic lake, including its meromictic nature, relatively high surface area/depth ratio (surface area ~ 0.1 km^2; $z_{max} = 30$ m), and steep margins, facilitated deposition and preservation of finely laminated facies, punctuated by clastic layers corresponding to turbidite events. The robust age model is based on 17 AMS ^{14}C dates. Slope instability caused large gravitational deposits during the middle Holocene, prior to 6 ka BP, and in the late Holocene, prior to 1,600 and 1,000 cal yr BP). Relatively shallower lake conditions prevailed during the middle Holocene (6,000–3,500 cal years BP). Afterwards, deeper environments dominated, with deposition of varves containing preserved calcite laminae. Increased carbonate production and lower clastic input occurred during the Iberian-Roman Period, the Little Ice Age, and the twentieth century. Although modulated by climate variability, changes in sediment delivery to the lake reflect modifications of agricultural practices and population pressure in the watershed. Two episodes of higher clastic input to the lake have been identified: 1) 690–1460 AD, coinciding with an increase in farming activity in the area and the Medieval Climate Anomaly, and 2) 1770–1950 AD, including the last phase of the Little Ice Age and the maximum human occupation in late nineteenth and early twentieth centuries.

Keywords Lake Montcortès · Western Mediterranean · Pyrenees · Holocene · Varves · Human impact · Little Ice Age

J. P. Corella (✉) · A. Moreno · M. Morellón · M. T. Rico · A. Pérez-Sanz · B. L. Valero-Garcés
Instituto Pirenaico de Ecología (CSIC), Avda. Montañana 1005, 50059 Zaragoza, Spain
e-mail: pablocorella@ipe.csic.es

V. Rull
Institut de Botànic de Barcelona (CSIC), Passeig del Migdia s/n, 08038 Barcelona, Spain

S. Giralt
Instituto de Ciencias de la Tierra Jaume Almera (CSIC), C/Lluís Solé i Sabarís s/n, 08028 Barcelona, Spain

Introduction

Recent studies have revealed large hydrological variability in the Mediterranean Basin during the Holocene, with complex fluctuations between arid and humid periods in response to changes in orbital configuration and insolation (Liu et al. 2006; Magny 2006) and Atlantic Ocean dynamics, i.e. North Atlantic Bond Cycles (Bond et al. 2001). The last few millennia are of particular interest because the main boundary conditions have been similar to present-day climate configurations and detailed regional palaeoclimatic reconstructions can be compared to current climate change processes.

In the Iberian Peninsula, the number of available Holocene lacustrine records has greatly increased in the last few decades. However, most of the records lack the chronological resolution to resolve sub-millennial variability during the Holocene. Paleohydrological fluctuations have been described in several late Holocene Spanish lacustrine records: Zoñar Lake (Martín-Puertas et al. 2008), Taravilla Lake (Moreno et al. 2008), Estanya Lake (Morellón et al. 2008), Lake Redon (Pla and Catalan 2005), and they seem to reflect regional climate impacts, particularly the 4 ka BP aridity crisis, the Iberian-Roman Humid Period, the dry and warm Medieval Climate Anomaly, and the cold and sometimes humid Little Ice Age.

Precise dating of Holocene climate fluctuations in the Iberian Peninsula has not yet been accomplished. Nor is the regional variability or interaction of climate changes with intense human impact in lake watersheds since Neolithic times, particularly during the last two millennia, well known. To understand Holocene hydrological variability in the western Mediterranean area, more reconstructions with adequate dating and sampling resolution are required, and in the Iberian Peninsula, karstic lakes may provide such records. The small size of perennial, freshwater, karstic lakes, along with the topographically closed nature of their basins and their connections to aquifers, make these lacustrine systems very sensitive to regional hydrologic changes. This type of lake experiences considerable water level fluctuations, as well as shifts in water chemistry and biology in response to changes in effective moisture (Cohen 2003). Sediment sequences from karstic lakes in Spain also record the impact of human activities during past centuries, such as Lake Chiprana (Valero-Garcés et al. 2000) and Lake Zoñar (Valero-Garcés et al. 2006), and even millennia, like Estanya Lake (Morellón et al. 2009), Lake Zoñar (Martín-Puertas et al. 2008, 2009), and La Cruz Lake (Romero-Viana et al. 2008), among others. Most karstic lakes in Spain are circular basins with step margins, and have a relatively high depth/area relationship, favouring thermal stratification. Permanent meromixis, however, is found in only a few lakes on the Iberian Peninsula (Miracle et al. 1992). The meromictic nature of these lakes and the strong seasonality of the Mediterranean climate, together with the occurrence of algal blooms in spring, are conducive to the genesis and preservation of varved sediments, as in Lake La Cruz (Julià et al. 1998; Romero-Viana et al. 2008) and Lake Zoñar (Martín-Puertas et al. 2009).

In this study, we investigated the finely laminated sediment sequence of Lake Montcortès, a karstic, deep (z_{max} = 30 m), meromictic lake in the Pre-Pyrenean Mountains spanning the last 6,000 years. This paleoenvironmental reconstruction is based on sedimentological, mineralogical and compositional analyses of four sediment cores retrieved from the deepest area of the lake and an age model constrained by 17 AMS ^{14}C dates. Finely laminated facies and annual varves dominate the record and allowed identification of periods of increased clastic input, changes in limnological and hydrological conditions related to climate variability and human impact in the watershed.

Study site

Geography and geology

Lake Montcortès (42° 19′ N, 0° 59′ E, 1,027 m a.s.l.) is a karstic lake located in the Pre-Pyrenean Range, NE Spain (Fig. 1a). The lake sits on the northern boundary of the tectonic South Pyrenean Central Unit, dominated by Mesozoic and Tertiary carbonate rocks and a number of thrust sheets affecting Paleozoic formations (Rosell 1994). Bedrock of the small lake catchment is composed of Triassic materials such as carbonates (Muschelkalk facies), claystones, and evaporites (Keuper facies) with some intrusions of hypovolcanic ophite bodies (Rosell 1994) (Fig. 1b). Presence of Muschelkalk limestones and dolostones, Oligocene carbonate conglomerates, and Triassic gypsum-rich materials (Keuper facies) favoured karstic development, leading to formation of depressions in the area by dissolution and collapse. This is similar to the process that gave rise to lakes in other Pre-Pyrenean zones, such as Estanya Lake (Morellón et al. 2008), Arreo Lake (Miracle et al. 1992) and Banyoles Lake (Canals et al. 1990).

The region has a Continental Mediterranean Alpine climate. Mean annual precipitation and temperature are 860 mm and 10.6°C, respectively.

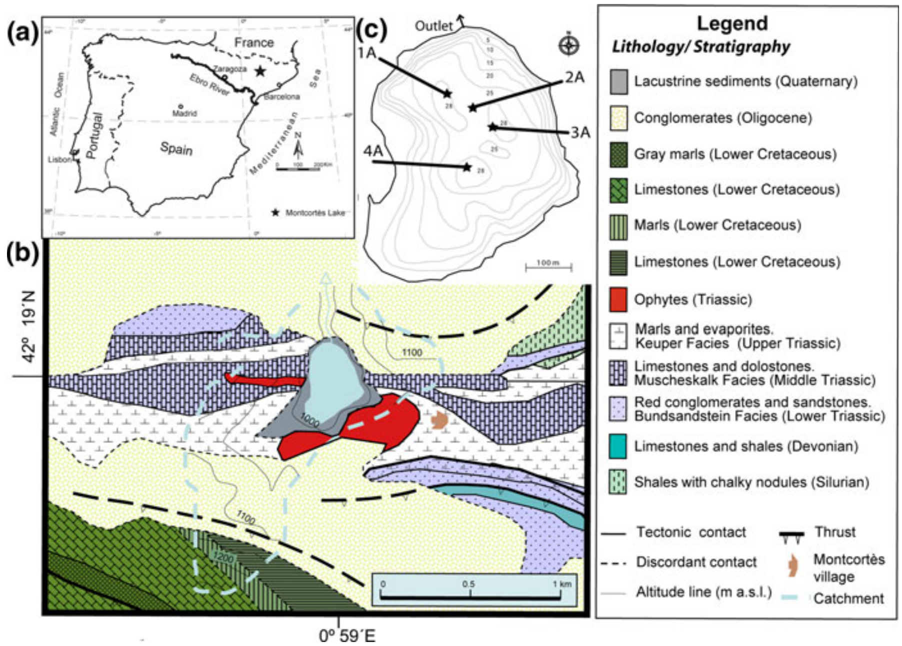

Fig. 1 **a** Geographic location of Montcortès Lake. **b** Geological map of the area surrounding Montcortès Lake. **c** Bathymetric map and location of the four Kullenberg cores retrieved: *1A*, *2A*, *3A* and *4A*

Monthly mean temperatures range from 1.9°C in January to 20.3°C in July. March is the driest month and May is the wettest, with mean rainfalls of 46.6 and 99.2 mm, respectively, as reported by the Senterada Meteorological Station, 5 km west of the lake.

The regional vegetation is Submediterranean and is dominated by *Buxo-Quercetum pubescentis* communities. The forest formations reflect a transition between the Mid-European and Mediterranean ecosystems, with trees dominated by *Quercus* and *Pinus* and shrubs dominated by *Buxus sempervirens*. Farm land with cereal crops and meadows cover flat areas (Blanco et al. 1997). Today, the lake shorelines are colonized by hygrophyte communities of *Juncus* sp., *Scirpus* sp., *Phragmites communis*, *Typha latifolia* and *Sparganium* (Camps et al. 1976).

Hydrology and limnology

Lake Montcortès' catchment belongs to the Flamisell River watershed. The lake is almost circular [maximum length = ~525 m, maximum width = ~450 m). Total shoreline length is 1,320 m and maximum water depth is 30 m (Camps et al. 1976)] (Fig. 1c).

There is no permanent inlet, but ephemeral creeks drain the southern area of the catchment, providing water and clastic sediments to the lake. An outlet stream, located on the north shore is currently inactive (Camps et al. 1976), although it functions during humid periods, thereby controlling lake level. Lake hydrology is mostly governed by groundwater inputs, including several springs and seepage from the main Triassic Muschelkalk aquifer and by outputs via the ephemeral outlet, groundwater and evaporation. Groundwater and lake waters have a similar chemistry dominated by HCO^{3-}, Ca^{2+} and Mg^{2+}. Similar conductivities were measured in nearby springs (from 278 to 1,420 µs/cm) and lake waters (average 372 µs/cm). Slight enrichment of sulphate in the lake waters relative to the springs is consistent with shale and gypsum-rich aquifers (Bayarri, pers. commun.), and also reflects evaporative concentration processes in the lake.

The lake is oligotrophic and meromictic, with permanently anoxic conditions in the monimolimnion below 18 m in summer and 20 m in winter, leading to high ammonium and sulphide concentrations, the latter favoured by sulphate-reducing bacteria (Camps et al. 1976). Transparency is relatively high, and 10% of surface irradiation reaches 5 m water depth from November to March. The thermocline shows gradients >1°C/m during summer. Alkalinity values range between 2.5 and 3.5 meq/l and pH is between 7.0 and 8.5 (Camps et al. 1976). Permanent anoxia in deep waters favours the preservation of finely laminated sediments in central-distal areas of the lake basin, as demonstrated by short gravity cores retrieved in 2007 and 2008. Littoral sediments are composed of massive carbonate silts with abundant plant remains and ostracods.

Materials and methods

Four Kullenberg cores were retrieved in May 2004 from the deepest area of the lake (Fig. 1c) using coring equipment and a platform from the Limnological Research Center (LRC, University of Minnesota). Cores MON04-1A-1K, MON04-2A-1K and MON04-3A-1K were located in a NW–SE transect in the northern part of the basin. Core MON04-4A-1K was taken in the southern part of the deepest area of the lake. The sediment–water interface was not preserved in these Kullenberg cores, but the uppermost part of the lacustrine sedimentary infill was recovered using gravity cores in 2007 (MON07-1A-1G, 31 cm long). The cores were split in half lengthwise and imaged with a DMT core scanner. Physical properties were measured every 5 mm with a Geotek multi-sensor core logger (MSCL) at the LRC. Cores were correlated using physical properties and sedimentary facies. Several gravitational deposits were identified in the cores. The MON04-1A-1K and MON04-4A-1K cores were selected to reconstruct the continuous sedimentary sequence and to carry out detailed compositional and mineralogical analyses.

The MON04-1A-1K core (6.69 m long) was sampled every 2 cm for total carbon (TC), total organic carbon (TOC), total sulphur (TS) and total nitrogen (TN). It was sampled every 5 cm for mineralogical analyses. The MON04-4A-1K core (5.38 m long) was sampled every 5 cm for the same analyses. The TC, TS and TOC were analyzed with a LECO 144DR elemental analyser. TIC values were obtained by subtracting TOC values from corresponding TC values. TN values were obtained with a VARIO MAX CN elemental analyser. Mineralogical analyses were carried out by X-ray diffraction (XRD), using an automatic X-ray diffractometer SIEMENS-D500, Cu-Kα, 40 kV, 30 mA and graphite monochromator. Identification and quantification of the mineralogical species in the crystalline fraction followed standard procedures described in Chung (1974a, b).

Sedimentary facies were defined visually, with microscopic smear slides, and with thin sections, combined with the results of compositional and mineralogical analyses (Schnurrenberger et al. 2003). Large-scale thin sections (120 mm $\times$ 35 mm) were prepared after freeze-drying, followed by impregnation with epoxy resin (Araldite) under vacuum. Representative samples of the different facies were selected for morphological description and mineralogical identifications using SEM–EDS with a JEOLJSM 6400 microscope coupled with an EDX analyser working at 20 kV and a 50 s analysis time.

In order to carry out the statistical treatment of the dataset (Principal Component Analysis, PCA), both magnetic susceptibility and compositional data were re-sampled every 5 cm to obtain a homogeneous database. The data, a matrix of 17 variables and 1129 cases, were normalised to eliminate effects due to large differences in the range of values for different variables.

The chronology of the Lake Montcortès sediment sequence was built using 17 AMS radiocarbon dates on bulk organic matter and terrestrial remains. Analyses were carried out at the Poznan Radiocarbon Laboratory (Poland) and the Lawrence Livermore National Laboratory (USA) (Table 1). Radiocarbon dates were calibrated using the INTCAL 04 calibration curve (Reimer et al. 2004). The age model was generated by linear interpolation of selected ^{14}C dates using *Analyseries 2.05* software (Paillard et al. 1996).

Results

Sedimentary facies

Six facies were defined in the cores: 1) finely laminated (facies 1 and 2); 2) banded (facies 3); 3) graded, turbidite-like (facies 4); and 4) gravitational deposits (facies 5 and 6) (Table 1). One of the most conspicuous characteristics of the Montcortès sediment sequence is its finely laminated nature, with two types of facies, distinguished by the presence (facies 1) or absence (facies 2) of calcite laminae. Facies 1 is composed of mm-thick triplets of three laminae: (a) white layers, mostly composed of 4–20-µm-long, euhedral calcite crystals, (b) greenish-brownish, organic-rich laminae with abundant diatoms and amorphous organic matter, and (c) grey laminae made up of carbonate, clay minerals and quartz particles of silt and clay size. Gray laminae are not

Table 1 Main sedimentological, mineralogical and geochemical (TIC, TOC, TS and C/N range values) features and inferred depositional environments for the Montcortès Lake sedimentary facies

	Facies	Sedimentological, mineralogical and geochemical features	Depositional environments
Laminated facies	1	*Variegated, finely laminated varves* Triplets composed of mm-thick laminae: i) white of endogenic calcite, ii) brown, organic with abundant diatoms and iii) grey of carbonate silt with quartz. TIC = 0.82–9.91%, TOC = 1.13–8.2%, TS = 1.23–6.73%, C/N = 9.43–11.05%	Offshore, anoxic hypolimnion, calcite precipitation in the epilimnion
	2	*Finely laminated facies with greenish, organic clay-rich and greyish detrital layers* Couplets of mm-thick laminae: i) brown to greenish, with high amorphous aquatic organic matter content, diatoms and clay minerals and, ii) grey composed of carbonate silt with quartz. Higher clay mineral and pyrite content than facies 1. White layers of endogenic calcite are scarce. Presence of partially dissolved gastropod shells and gastropod shell moulds TIC = 0.45–0.99%, TOC = 5.23–17.9%, TS = 2.41–6.81%, C/N = 12.6–14.41%	Shallow lake, high bioproductivity, anoxic and more acidic hypolimnion
Banded facies	3	*Banded, brownish and greyish carbonated facies littoral facies* Alternating cm-thick: i) brown layers of carbonate silty mud with organic matter, gastropod fragments, and ii) grey layers of carbonate silt with quartz. In subfacies 3.1 brown layers dominate while in subfacies 3.2 grey layers dominate. TIC = 2.94–8.93%, TOC = 2.2–9.77%, TS = 1.22–7.95%, C/N = 10.51–16.5%	Littoral
Graded facies	4	*Graded detrital layers* Cm-thick fining upward sequences composed of carbonate silty mud with quartz, feldspar and clays and massive, blackish finer silty mud. Facies with highest magnetic susceptibility TIC = 0.4–1.05%, TOC = 1.49–2.09%, TS = 0.34–3.61%, C/N = 10.32–11.86%	Proximal and distal deposits from turbidity processes
Gravitational deposit facies	5	*Convoluted and disrupted facies* Laminated facies with convoluted textures affected by folds, microfractures and microslides.	Gravitational processes affecting lacustrine sediments
	6	*Massive, conglomeratic facies* Chaotic facies with centimetric sandstone and limestone clasts within a sandy matrix and cm- to dm-thick dark grey quartz silts with abundant plant remains and limestone clasts.	Gravitational processes affecting alluvial/colluvial deposits

always present. Facies 1 displays intervals with thicker detrital grey laminae and more frequent deposition of intercalated massive layers, coinciding with peaks in the magnetic susceptibility (MS), and intervals showing thicker calcite laminae, thinner clastic laminae and less frequent massive clastic facies (Fig. 2).

Scarce bioturbation textures in laminated facies indicate limited bottom biological activity as a consequence of anoxic conditions (Brauer 2004). In small, relatively deep karstic lakes with fluctuating water levels, these conditions occur during meromictic phases that usually correspond to periods of relatively higher lake levels (Brauer 2004; Martín-Puertas et al. 2009). The characteristics of these triplets suggest they represent an annual cycle in lake deposition, with calcite formation in the epilimnion during the warmest seasons associated with algal blooms (spring and summer), deposition of organic matter and diatoms during summer and fall (a brownish-greenish layer), and clastic material deposited during the rainy seasons in late fall and winter or

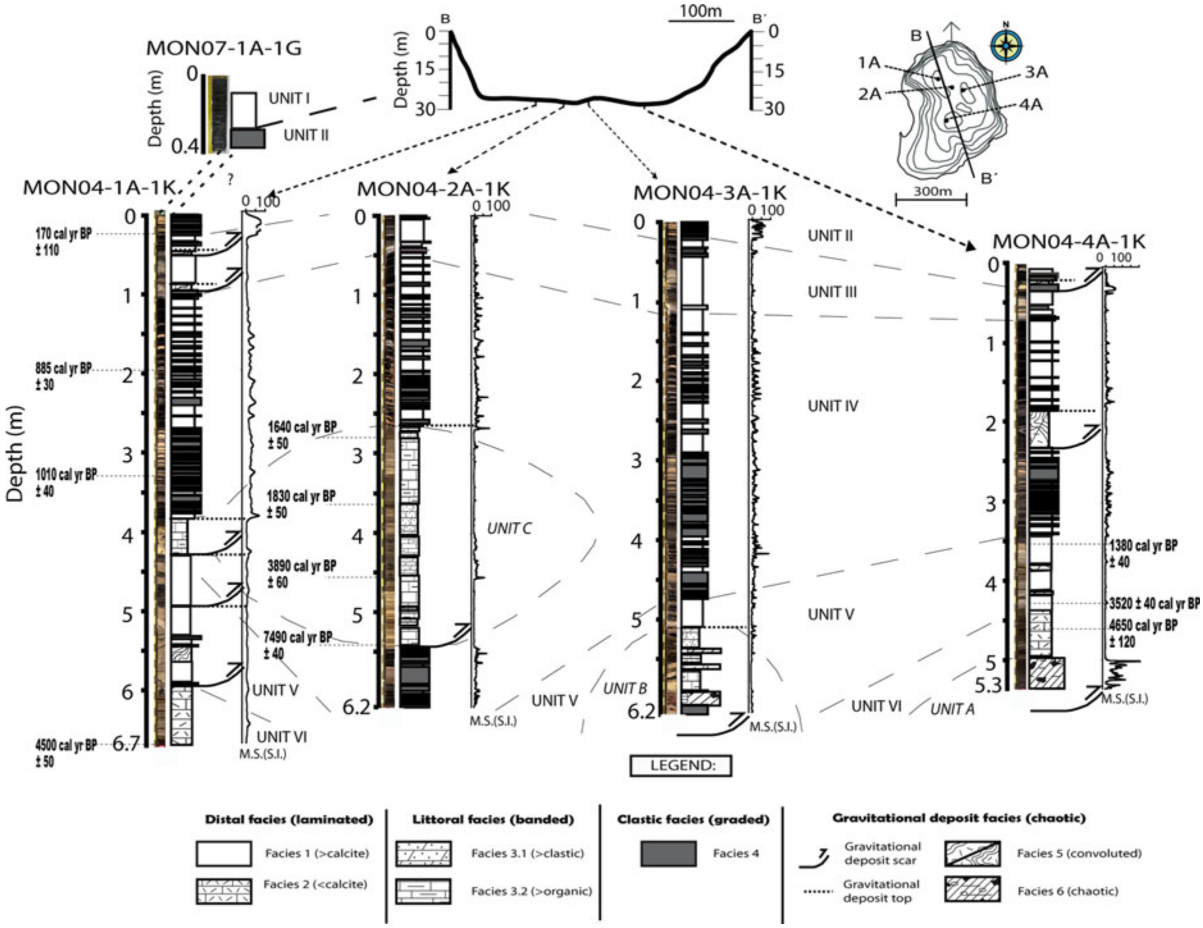

Fig. 2 Lithostratigraphic correlation of the four cores. Each core image is accompanied by its sedimentological description and magnetic susceptibility values. *Dashed lines* represent the correlation between the main sedimentary units. The depth of the AMS ^{14}C dates is also indicated

during storm events. These phenomena also occur in other lakes on the Iberian Peninsula, e.g. Zoñar Lake (Martín-Puertas et al. 2009); La Cruz Lake (Julià et al. 1998), and elsewhere, e.g. Piànico-Sèllere Basin (Mangili et al. 2007), and Elk Lake in the US (Anderson and Dean 1988). Intervals of facies 1 with thicker detrital grey laminae are interpreted as higher clastic input to the lake during autumn and spring rains. The presence of intervals with thicker calcite and organic laminae points to periods of enhanced biological productivity in the epilimnion that allow precipitation and preservation of endogenic calcite laminae. Facies 1 is similar to modern sediments in the deepest areas of the lake.

Facies 2 is composed of couplets of two laminae: (1) mm-thick, brown to greenish, organic-rich laminae with higher content of amorphous aquatic organic matter, diatoms and clay minerals, and (2) mm-thick terrigenous grey layers of silt composed of clay minerals, carbonate and quartz particles. Facies 2 has the highest TOC values in the sediment sequence (up to 18%) and thicker diatom- and organic matter-rich laminae, suggestive of high biological productivity and organic matter preservation in the lake. However, high C/N ratios, up to 15.5%, indicate predominance of terrestrial over aquatic plants as the source of organic matter (Meyers 2003), and the clay content (66–88%) points to high clastic input to the lake. The absence of calcite laminae indicates that conditions were not adequate for precipitation of calcite in the epilimnion and/or preservation in the sediments. The lake bottom and sediments could have been strongly reducing as suggested by the high organic matter and botryoidal pyrite content (up to 4%), leading to the inhibition of calcite precipitation or to its dissolution (Dean 1999). Presence of gastropods and mollusks indicates relatively more littoral settings. All these sedimentary features point to relatively shallow-water conditions during deposition of facies 2, with high detrital and organic input from the watershed and high organic productivity in the lake.

Banded, carbonate facies 3 is composed of cm-thick, greyish-brownish layers of terrigenous, carbonate, silty mud with organic matter, with abundant *Chara* and gastropod fragments, indicative of deposition in carbonate-producing littoral environments. Subfacies 3.1 is dominated by grey, silty, carbonate layers, pointing to higher clastic input from the drainage basin and reworking of carbonates in the littoral platform, while subfacies 3.2 is richer in organic matter.

Facies 4 occurs as cm- to dm-thick (up to 11.2 cm thick) layers, with fining-upward textures, erosive basal surfaces with plant remains, a sandy basal layer with some gypsum crystals, carbonate fragments and coarse quartz grains, and a graded layer of silt to fine mud. This facies has the highest MS values. The sedimentological features of facies 4 are characteristic of turbidite-type or storm-related deposits (Noren et al. 2002). The graded nature indicates deposition by turbidity currents that separate the coarse bed load from the fine grains in suspension. Irregular detrital gypsum crystals occur only in the basal clastic sublayer.

Principal Component Analysis (PCA) was applied to the compositional matrix (elemental, mineralogical and MS data) to investigate the main environmental processes controlling sediment deposition (Giralt et al. 2008). The two main eigenvectors accounted for 58.75% of the total variance (Fig. 3). The first eigenvector (PCA 1) represents 36.2% of the total variance and is controlled by dolomite, Mg-calcite and quartz at the positive end and by TS, TOC, TN, C/N and pyrite at the negative end (Fig. 4). The association of Mg-calcite and dolomite with quartz suggests that these minerals are mainly detrital, eroded from the carbonate and evaporite of the Keuper and Muschelkalk formations that outcrop in the drainage basin. The first eigenvector is likely reflecting periods of increased primary productivity (negative values), anoxic conditions, and early diagenetic processes leading to pyrite formation, as opposed to periods of increased clastic delivery to the lake (positive values).

The second eigenvector (PCA 2) represents 22.55% of the total variance and is tied to calcite and TIC at the positive end and to magnetic susceptibility and silicates (feldspars, micas and clays) at the negative end. This eigenvector shows the opposite relationship between the deposition of a distal, fine-grained siliciclastic fraction and precipitation of endogenic carbonates.

Gravitational deposits from several dm to 3 m thick were identified in the Montcortès sequence. They are more abundant in the lower part of the record and the thickest gravitational deposit can be correlated across different cores. Most of them are limited by slide surfaces, and show little to no internal deformation. Facies within the gravitational deposit intervals were assigned to the different facies identified above and were described according to their sedimentological characteristics, independent of their position in the allochthonous units. Only intervals with strong deformation structures were described as gravitational deposit facies: (1) facies 5 is a laminated facies with convoluted textures, folds, microfractures and slides; and (2) facies 6 is a

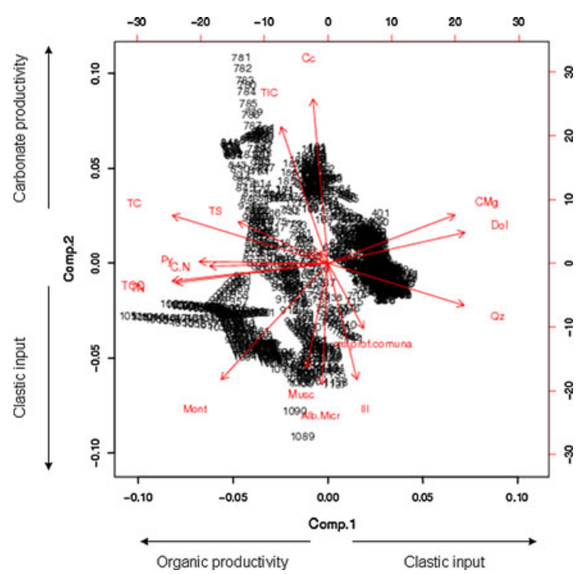

Fig. 3 Principal Component Analysis (PCA) carried out with the geochemical (TIC, TOC, TS, TN and C/N), mineralogical and MS data from the Montcortès Lake sequence. The *arrows* represent the analyzed variables and numbers indicate the position of every sample. Eigenvector 1: standard deviation = 24.089, proportion of the Variance = 0.362, cumulative proportion = 0.362; Eigenvector 2: standard deviation = 19.578, proportion of the Variance = 0.225, cumulative proportion = 0.587

massive, chaotic heterometric deposit with abundant mm- to cm-long angular limestone and sandstone clasts and plant remains in a quartz-rich and silty matrix.

Core correlation and stratigraphy

The composite sequence of the Montcortès record was constructed using the uppermost part of core MON04-1A-1K (0–357 cm) and the lowermost part of core MON04-4A-1K (357–569 cm), both close to the western margin of the basin, and the gravity short core, MON07-1A-1G (Fig. 4). The Lake Montcortès sediment sequence was divided into six main litho-stratigraphic units (I–VI) and three allochthonous units (A, B and C) (Fig. 2).

Unit VI (532–470 cm) only occurs in the MON04-1A-1K and MON04-4A-1K cores and is made up of facies 2 and characterized by an upcore parallel decrease in organic carbon and clay mineral content (Fig. 3). The upper limit is defined by an increase in the abundance of endogenic calcite laminae.

Units V (470–377 cm), III (109–31 cm) and I (24–0 cm, MON07-1A-1G) group variegated, finely laminated and carbonate-rich sediment (facies 1). In both units V and III, detrital layers are more abundant at the base (subunit V.c and subunit III.b), while calcite layers are more common at the top (subunit V.a and III.a). Unit V has a 15-cm-thick interval of facies 2 (sub-unit V.b) and several interbedded gravitational deposits in the MON04-1A-1K and MON04-3A-1K cores (Fig. 2).

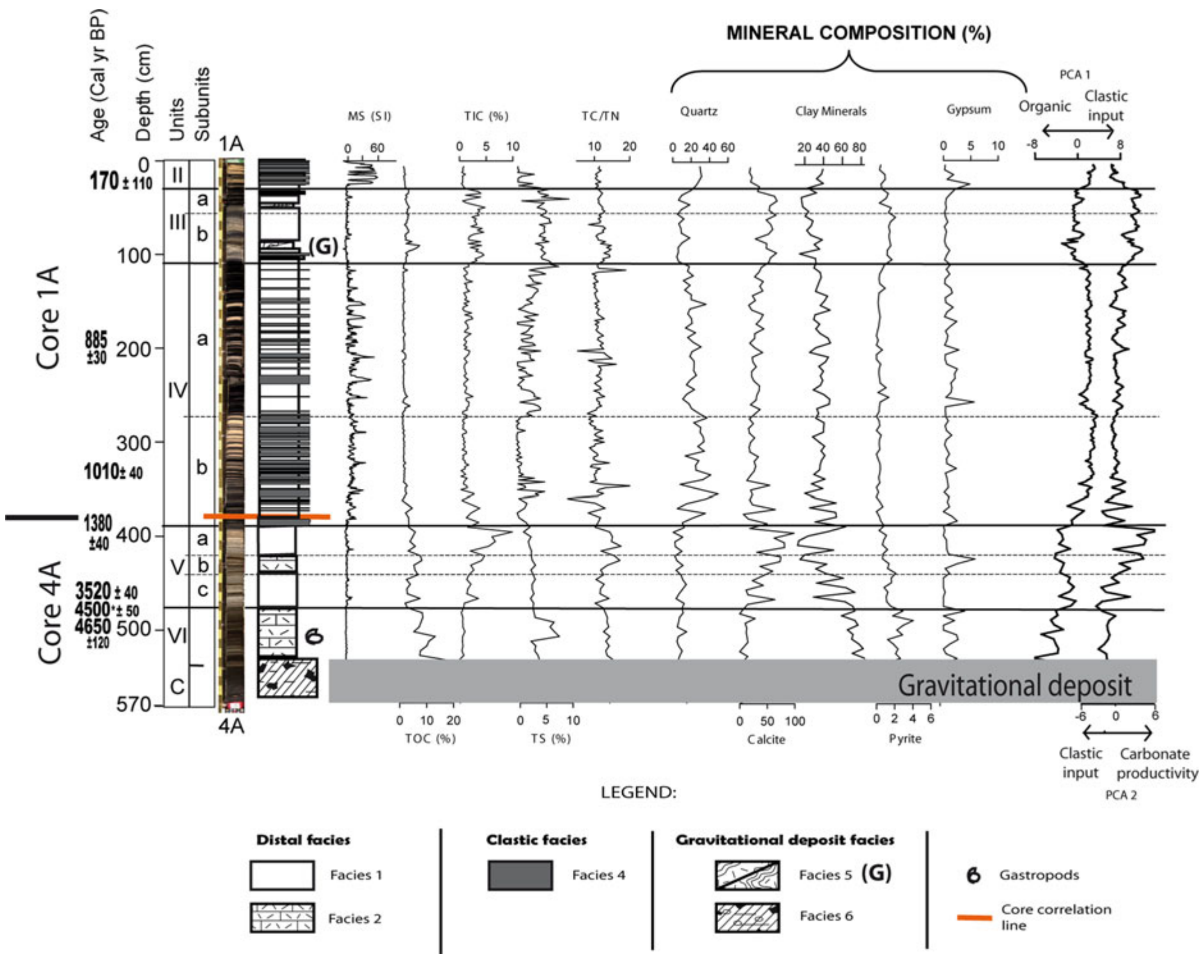

Fig. 4 Sedimentological, compositional and mineralogical profiles from the lithostratigraphic units and subunits defined in cores MON04-1A-1K and MON04-4A-1K. AMS ^{14}C dates are indicated on the *left* side of the figure

Units IV (377–109 cm) and II (31–24 cm) are black and grey, banded to laminated sediments (facies 1), with abundant turbidite beds (facies 4). Turbidite presence decreases from the base (subunit IV.b, 377–109 cm) to the top of unit IV (subunit IV.a). This unit contains several gravitational deposits, present in all the cores except MON04-3A-1K (Fig. 2). Unit II has sharp upper and lower limits marked by the transition between graded facies 4 and laminated facies 1.

The subunits with higher detrital content (units V.c, IV and II, Fig. 4) have the highest and lowest values of PCA 1 and 2, respectively. The eigenvectors show opposite behaviour in the units with higher carbonate (units I, III) and organic (unit VI) contents (Fig. 4).

Several major gravitational deposits, limited by surfaces with deformation and slide structures, were identified in the Montcortès sequence (units A, B and C). The thickest ones occur in cores MON04-2A-1K and MON04-3A-1K, close to the northeastern margin of the lake (Fig. 2). They are composed of littoral, banded, carbonate-rich sediments (units B and C, facies 3) and may include even cm-long clasts of Triassic (Muschelkalk facies) and Tertiary (Oligocene) rocks (units A and B, facies 5 and 6). The oldest gravitational deposit occurs in core MON04-4A-1K (unit A), and includes chaotic, heterometric clastic facies with limestone and sandstone clasts. The thickest gravitational deposit (Unit C, 280 cm) is located within unit IV in the MON04-2A-1K and MON04-1A-1K cores, and affected banded, carbonate-rich littoral sediments (facies 3) deposited in the north-eastern platform of the lake. The gravitational deposit registered in core MON04-3A-1K (unit B), assigned to unit V, also includes littoral, carbonate-rich sediments (facies 3) and could correlate with some of the gravitational deposits observed in the MON04-1A-1K core.

Age model

The chronology of the Montcortès sequence is based on 17 AMS ^{14}C dates from three cores (Table 2). The age model of upper units I to IV is constrained by

Table 2 Radiocarbon dates obtained in the Montcortès Lake MON04-1A-1K, MON04-2A-1K and MON04-4A-1K cores

Core depth (m)	Lab code	Material	^{14}C year BP	Cal years BP (2σ range)	Unit	Facies
MON04-1A-1K						
0.29	Poz-23689	Aquatic rest	180 ± 30	170 ± 110	II	4
2	Poz-23650	Macrorest	885 ± 30	830 ± 60	IV	4
3.34	Poz-23651	Macrorest	1,080 ± 30	1,010 ± 40	IV	4
6.69	Poz-9812	Macrorest	4,030 ± 35	4,500 ± 50	VI	2
MON04-2A-1K						
2.77	Law-86494	Charcoal + seeds	1,715 ± 35	1,640 ± 50	C	3
3.64	Poz-31027	Macrorest	2,260 ± 40	1,830 ± 50	C	3
4.57	Law-144044	Charcoal	3,950 ± 30	3,890 ± 60	C	3
5.44	Law-86495	Charcoal + seeds	6,580 ± 35	7,490 ± 40	C	3
MON04-4A-1K						
0.72	Poz-13036	Bulk sediment	1,290 ± 35	1,240 ± 40*	IV	4
3.55	Poz-13035	Bulk sediment	1,485 ± 50	1,380 ± 40	V	1
4.31	Poz-23652	Macrorest	3,285 ± 30	3,520 ± 40	V	1
4.62	Poz-23713	Macrorest	4,090 ± 40	4,650 ± 120	VI	2
4.99	Law-86496	Charcoal	2,585 ± 50	2,660 ± 100*	A	6
5	Poz-23690	Macrorest	6,600 ± 40	7,500 ± 40*	A	6
5.13	Poz-24949	Macrorest	8,010 ± 50	8,880 ± 100*	A	6
5.3	Poz-10328	Macrorest	6,740 ± 50	7,610 ± 40*	A	6
5.3	Poz-23771	Bulk sediment	10,470 ± 110	12,380 ± 200*	A	6

Ages labelled with an asterisk were not included in the age model. *N Law* Lawrence Livermore Laboratory; *Poz* Poznan Radiocarbon Laboratory

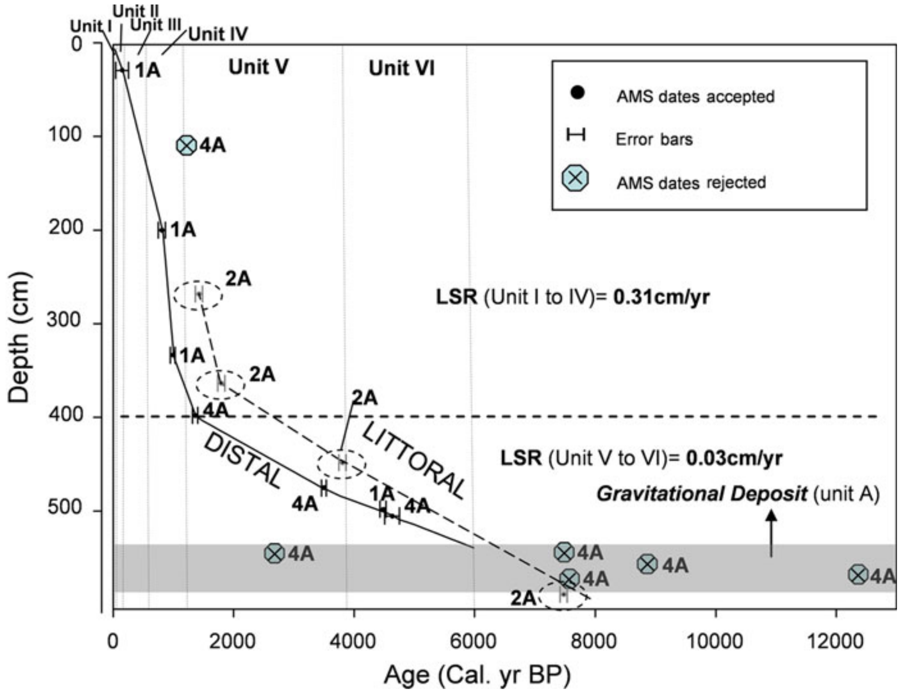

Fig. 5 Chronology of the sediment sequence based on linear interpolation of 16 AMS ^{14}C dates. Estimated sedimentation rates for two intervals are indicated. *Dashed line* represents the littoral sediment accumulation calculated using the four ^{14}C dates from core 2A. *Dashed ovals* circle AMS ^{14}C dates from littoral core 2A. *LSR* Linear Sedimentation Rate

three dates (two from terrestrial macrorests and one from an aquatic rest) in core 1A. Because the age of the aquatic rest (180 ± 30 ^{14}C yr BP) is similar to other ^{14}C dates and agrees with preliminary varve counting in unit I, the reservoir effect appears to be negligible in Montcortès. A sample from core 4A (unit III, 72 cm, 1,290 ± 35 ^{14}C yr) is too old, likely due to reworking of older lake deposits, and was rejected. Units V and VI were dated in cores 1A (1 date) and 4A (3 dates). Four samples (charcoal, seeds and macrorests) in the base, middle and the top of unit C were dated in core 2A. Five radiocarbon dates were obtained from unit A and they show a large range, as expected, due to the reworked, allochthonous nature of this unit. Most of the dates, however, are between 10,500 and 6,600 ^{14}C yr BP, suggesting that the unit includes early to middle Holocene sediments and that the gravitational process occurred during the middle Holocene.

The age of the base of the sequence was obtained assuming a constant sedimentation rate between units V and VI. According to this chronological model, the Lake Montcortès sediment sequence spans the last *ca*. 6,000 cal yr and the oldest in situ deposits are those in unit VI of core 4A (Fig. 5). The sedimentation rate is relatively low in units V and VI (0.03 cm/yr), increasing tenfold to 0.31 cm/yr during the last 1,300 years. This increase in sedimentation rate correlates with a change in the sedimentary facies and higher frequency of turbidites (facies 4 and 5). The emplacement of unit A would have occurred prior to 6,000 cal yr BP. Unit B was emplaced during the early deposition of Unit V, around 1,600 cal yr BP. Unit C records sedimentation in the littoral northeastern margin of the lake from *ca*. 7,500–1,640 cal yr BP. Littoral sedimentation rate displays a trend similar to that of distal deposits: a lower sedimentation rate during the interval 7,490–1,830 cal yr BP (0.03 cm/yr) and an abrupt increase after 1,830 cal yr BP (0.45 cm/yr). Detailed correlation between cores 1A and 2A suggests the gravitational deposit that transported these littoral materials to the deep areas of the lake occurred during deposition of unit IV, just after ~1,000 cal yr BP (Fig. 2).

Discussion

Depositional evolution of Montcortès Lake

Four main depositional stages were identified during the last 6,000 cal yr BP in Lake Montcortès based on sedimentary facies analysis and core correlation (Fig. 6):

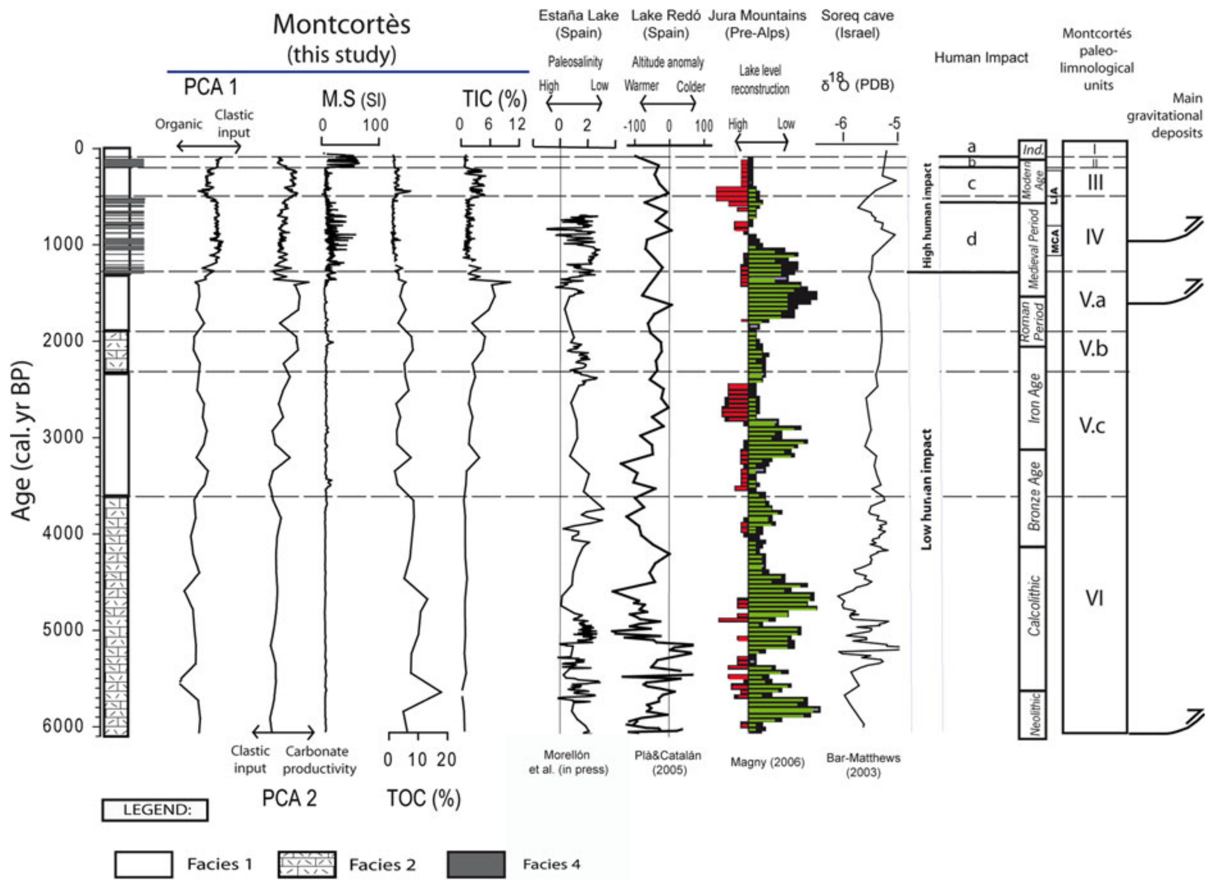

Fig. 6 Depositional evolution of Montcortès Lake during the last 6,000 cal yr based on selected proxies and comparison with other Iberian and Mediterranean paleorecords. From *left* to *right*: Sedimentary facies; *PCA 1* first main eigenvector, *PCA 2* second main eigenvector, *M.S.* Magnetic susceptibility, *TOC* total organic carbon, *TIC* total inorganic carbon; Estanya Lake paleosalinity record (Morellón et al. 2008); Lake Redon altitude anomaly reconstruction (Pla and Catalan 2005); Mid-European lake level reconstruction, black boxes represent the 2σ range of radiocarbon dates (Magny 2006); $\delta^{18}O$ per mil in Soreq Cave speleothem record (Israel) (Bar-Matthews et al. 2003); human impact periods **a** massive emigration since mid twentieth century; **b** maximum population during the nineteenth century; **c** Late medieval economic crises and depopulation; **d** medieval increase in population, abundant fires and permanent land exploitation; historical periods (Roman, Medieval, Modern and Industrial),; paleolimnological units and main gravitational deposits

(1) Early Holocene (prior to 6,000 cal yr BP, unit A): Gravitational processes and littoral lacustrine and alluvial/colluvial sediments

Prior to 6,000 cal yr BP, a gravitational deposit, containing lacustrine sediments and some coarse clastic materials of alluvial or littoral origin, was emplaced in the southern end of the lake (unit A). Although the sediments are reworked and depositional textures and structures are not easily recognizable, the clastic nature of the facies (68–96% silicates), and the presence of large clasts, suggest that the sediments were originally deposited in a shallow, littoral lacustrine setting with alluvial influence.

(2) Middle Holocene (6,000–3,800 cal yr BP; 4090–1850 BC; Unit VI): relatively shallow, meromictic lake with a carbonate platform and associated palustrine subenvironments

Finely laminated facies 2 covered Unit A, suggesting an anoxic lake bottom where the gravitational deposit was emplaced. Fine laminations and development of diatom-rich and organic-rich laminae suggest high primary productivity and good preservation potential in the anoxic western and southern deep areas of the lake (Unit VI, core 4A: 500–438 cm, core 1A: 670–600 cm). Organic matter accumulation decreased progressively, reaching a minimum at the end of this stage. Intervals with thicker and more frequent clastic laminae define periods of higher sediment delivery to the lake. There is some evidence to suggest a relatively shallow depositional environment: (1) high C/N ratio, indicative of relatively greater terrestrial plant input than lacustrine organic matter input (Meyers 2003); (2) abundance of typical littoral biota, like gastropods and ostracods: (3) presence of layers composed of reworked lacustrine carbonate, indicating proximity of the littoral platform.

Although there are no calcite laminae in facies 2, carbonate productivity was very high in the north-eastern littoral shelf, as banded carbonate facies 3 deposited during this period (Unit C). The nature of facies 3, with abundant *Chara* fragments, demonstrates the development of a large carbonate shelf during the Holocene in the NE margin of Montcortès Lake. This platform was likely the source of the carbonate particles that reached the deepest areas and intercalated within facies 2. The development of large charophyte meadows would have also acted as a barrier to coarse sediments, allowing only the sedimentation of fine-grained particles and favouring enrichment of clay mineral content in facies 2. The absence of carbonate laminae in deeper environments is consistent with high accumulation of organic matter there. This would have led to lower pHs in anoxic pore waters, values sufficient to dissolve $CaCO_3$ particles reaching the sediment–water interface (Dean 1999).

In summary, Middle Holocene depositional environments in Lake Montcortès included a well-developed carbonate littoral shelf in the NE margin (facies 3.2), relatively deeper anoxic environments in the central and western areas, dominated by organic and fine clastic deposition (facies 2), and likely, a shallower, wetland area to the SW that could have been the source of organic matter to laminated facies 2 and also acted as a filter for coarse clastic particles.

(3) Late Holocene to Medieval Age (3,800–1,260 cal yr BP; 1850 BC–690 AD; Unit V): Deep, meromictic, carbonate-producing lake with high biological productivity

Higher lake levels, meromictic conditions, and a gradual increase in the biological productivity of the lake, with deposition of varved facies 1, prevailed in Montcortès Lake from 3,800 to 1,260 cal yr BP. Three periods can be differentiated according to the dominance of facies 1 (with endogenic calcite laminae) or facies 2 (without such laminae). During the first phase (3,800–2,350 cal. yr BP; 1850–400 BC, subunit V.c), deposition of thick and frequent clastic grey laminae indicate an increase in catchment runoff and sediment input to the lake that could have been associated with a lake level increase. The deposition of a 15-cm-thick, brown, organic-rich interval (facies 2) (2,350–1,910 cal yr BP; 400 BC–40 AD, subunit V.b) suggests a transition to depositional environments similar to unit VI, and likely, lower lake level. Finally, during the last phase of this stage (subunit V.a, 1,910–1,260 cal. yr BP; 40–690 AD), varves with calcite, organic and occasionally detrital laminae were deposited (facies 1), and calcite layers were particularly well developed. Formation of calcite may be controlled primarily by annual changes in biological productivity (Kelts and Hsü 1978), especially seasonal algal blooms, as have been described elsewhere (Romero-Viana et al. 2008). Primary productivity was high, as indicated by the high organic content, up to 8.2%, and low C/N ratios (Fig. 3) typical of lacustrine organic matter. The relation between algal activity and calcite precipitation has been documented in SEM images of monospecific diatoms in laminae, predominantly a centric, planktonic taxon, *Cyclotella sp*. (Scussolini, pers. commun.), associated with the calcite laminae. The inferred conditions for this period of calcite formation (subunit V.a) would have been similar to those in the lake today, i.e. relatively high lake levels, high carbonate and calcium input from the aquifers and surface waters, low sediment delivery, and a progressive increase in epilimnetic primary productivity.

Unit V shows several interbedded gravitational deposits in the MON04-1A-1K, MON04-2A-1K and MON04-3A-1K cores. The largest gravitational deposit in the sediment record (Unit C) was found in unit IV of the MON04-2A-1K (545–265 cm) and MON04-1A-1K (388–432 cm) cores. This gravitational process affected middle to late Holocene carbonate-rich littoral sediments deposited in the northeastern platform of the lake between 7,490 and 1,640 cal yr BP. The gravitational slide occurred *ca.* 1,010 yr BP (940 AD). In the carbonate shelf recovered in unit C, the onset of this stage at 3,800 cal yr BP corresponds with an abrupt increase in detrital input and a change to deposition of the more clastic, banded, carbonate facies 3.1. After this period, sedimentation in the platform, however, remained carbonate-rich, similar to previous stages.

The gravitational deposit registered in the MON04-3A-1K core (unit B) also includes littoral, carbonate-rich sediments and could correlate with some of the gravitational deposits observed in the lower part of the MON04-1A-1K core. Seismically induced structures like liquefaction levels or fault-graded beds (Rodríguez-Pascua et al. 2003) have been observed. These gravitational deposits probably originated along the northern margin of the lake. The relative chronology also indicates that this gravitational process occurred prior to 1,600 cal yr BP. Submerged, sediment-laden slope instability occurs in lacustrine environments, caused by increased erosion, high sedimentation rates, gas release or migration, seismic events, or hydrological fluctuations (Strasser et al. 2007). In the case of Lake Montcortès, rapid lake level fluctuations probably did not occur during this period, because the hydrological balance was controlled by the location of the outlet and no rapid changes of facies were detected.

(4) Last 1,300 years: Deep, meromictic lake with alternating phases of high clastic input and high carbonate productivity

The onset of this period was gradual, starting with deposition of facies 1 and an increase in silicate mineral content. During the first stage, corresponding to the Medieval Period (1260–490 cal yr BP; 690–1460 AD; Unit IV), laminated facies 1 was deposited, with frequent intercalations of turbidites (facies 4). The high turbidite frequency and the occurrence of the highest sedimentation rate in the whole sequence (3.1 mm/yr) underline the increase in sediment delivery to the lake. The frequency of turbidites greatly increased thereafter, during deposition of unit IV.a, and up to 490 cal yr BP (1460 AD). The turbidite layers in Montcortès Lake may correspond to single events characterized by a rapid influx of terrigenous sediments transported by runoff.

An abrupt decrease in clastic input signalled the onset of the following phase (490–180 cal yr BP; 1460–1770 AD), dominated by deposition of variegated, finely laminated carbonated facies 1 (unit III; Fig. 4). This phase with higher endogenic calcite formation and organic matter production, was especially intense during the last depositional stage (unit III.a).

Clastic input increased slightly after 280 cal yr BP (1660 AD) (Subunit III a), but the large limnological change occurred at about 180 cal yr BP (1770 AD) when turbidite processes dominated deposition in the central areas of the lake (fining upward sequences of facies 4 and high MS values, Unit II). The sedimentation rate increased again, as occurred in unit IV. Presence of gypsum associated with the detrital layers suggests reworking of littoral sediments or evaporite-bearing formations in the watershed. This period of increased clastic input continued during the nineteenth century. During the twentieth century, sedimentation of facies 1 with reduced clastic input, resumed (Unit I). Current depositional environments in Montcortès (unit I) are similar to those represented by subunits III.b and V.a: meromictic conditions with precipitation of endogenic carbonates during warm seasons associated with algal blooms.

Climate variability and human impact

The Montcortès record provides a case study of the synergistic effects of climate and human activities in Mediterranean mountain areas during the late Holocene (Fig. 6). During the middle Holocene (6,000–3,800 cal years BP; 4090–1490 BC), when lake levels were relatively shallower than during the late Holocene, human impact in the watershed was low. Most lacustrine (González-Sampériz et al. 2008; Morellón et al. 2008) and fluvial (Benito et al. 1996) records in the Iberian Peninsula show evidence of increased aridity in the middle Holocene compared to relatively more humid early and late Holocene times. Particularly, nearby Estanya Lake shows similar behaviour, with development of a saline, gypsum-rich lake, punctuated by periods of higher clastic delivery into the lake during this middle Holocene period (Morellón et al. 2008). And the higher altitude (2,240 m a.s.l.) record of Estany Redon (Central Pyrenees) shows a warming trend from the early Holocene to 4 ka BP (Pla and Catalan 2005) (Fig. 6). The onset of this period of higher aridity in the Iberian Peninsula at around 6 ka BP correlates with similar changes in the Alps (Magny 2006) and in northern Africa, with the end of the African Humid Period (Kropelin et al. 2008), and it has been interpreted as a reflection of decreasing summer solar radiation in the northern hemisphere.

A significant limnological change occurred in Montcortès at about 3,800 cal yr BP (1850 BC) when endogenic calcite that precipitated in the epilimnion was preserved in sediments and varves composed of three laminae were deposited. This period, interpreted in Montcortès as relatively more humid, lasted up to 2,350 cal yr BP and it corresponds with the cold and wet phase of the Iron Age in northern Europe (Leira 2005) between 3,000 and 2,000 cal yr BP (1050–50 BC), the onset of the humidity increase in the Mediterranean area (Sadori et al. 2004; Martín-Puertas et al. 2008, 2009) after the aridity crisis at 4.2 ka BP (Drysdale et al. 2006) and evidence of higher activity (2,865–2,350 cal yr BP) in the Spanish fluvial record (Benito et al. 2008). The interpreted Montcortès lake level drop between 2,350 and 1,910 cal yr BP (400 BC–40 AD) coincides with a reduction in river flood frequency on the Iberian Peninsula (Macklin et al. 2006) between 2,350 and 2,000 cal yr BP and lower lake levels in Zoñar Lake between 2,100 and 1,900 cal yr BP (Martín-Puertas et al. 2008).

The Iberian-Roman Humid Period (500 BC–400 AD) is well defined in southern Spain (Zoñar Lake) where it is the most humid phase during the last 4,000 years (Martín-Puertas et al. 2008). In the lake records from northern Spain, however, such as Estanya Lake (Morellón et al. 2008) and Estany Redon (Pla and Catalán 2005), the paleohydrological signal is not so clear. After 1,900 cal yr BP (50 AD), varves with endogenic calcite dominated in Montcortès until present day, indicating that lake level remained relatively high, controlled by the location of the outlet. This change correlates with an increase in lake level during the last 2,000 years, observed in other records from nearby lakes such as Estanya Lake (Morellón et al. 2008) in the Pre-Pyrenees or La Playa and La Salineta Lakes (González-Sampériz et al. 2008) in the Ebro Basin. The onset of this humidity increase coincides with the beginning of the Classic Roman Period that has been documented as a humid period in the Mediterranean area (Reale and Dirmeyer 2000) and with a second humid phase in the Zoñar Lake record (Martín-Puertas et al. 2008).

The period 1260–490 cal yr BP (690–1460 AD), with high clastic input in Montcortès Lake, coincides with the Medieval Climate Anomaly (MCA), a relatively warm and arid period in the Northern Hemisphere (Seager et al. 2007) that has been related to an increase in global irradiance (Bard et al. 2000). During that period, several Spanish lake records show evidence of aridity: (1) in the south (Zoñar Lake, between 1350 and 730 cal yr BP (600–1220 AD) (Martín-Puertas et al. 2008), (2) in the Pyrenees, Estanya Lake, between 950 and 800 cal yr BP (1000–1150 AD) (Morellón et al. 2008) and (3) in the Iberian Range, La Cruz Lake (Julià et al. 1998) and Taravilla Lake (Moreno et al. 2008). Likewise, there is an aridity increase during this period in lakes of central Italy (Dragoni 1998) and northern Africa (Lamb et al. 1995) and a decrease in the mean precipitation inferred in the Soreq Cave record, Israel (Bar-Matthews et al. 1999) (Fig. 6).

The increase in sediment delivery to the lake during medieval times is likely the result of a synergistic interaction between anthropic and climatic factors. The onset of this period coincides with the Muslim Conquest of the region in the seventh century AD, which brought greater regional development of farming practices, with new irrigation techniques, particularly in the valleys. During Medieval times, the Pyrenees and the southern slopes where Montcortès Lake is located, experienced an increase in population as a result of the migration of people escaping from the northward Muslim expansion, and continuous warfare in the lowlands. Once the Christian Kingdoms were established, fire was used commonly to prepare land for shifting cultivation, and forests were intensively used. During the tenth century, coinciding with deposition of subunit IV.b, more controlled and planned land exploitation was established, using livestock for ploughing and as a fertilizer source (see review in Rull et al. this volume). River margins and wetlands were preferred places for this type of mixed farming (Rull et al. this volume). Thus, the high sedimentation rate of unit IV may have been the result of a combination of climatic factors (increased high intensity storm events, relatively lower lake levels, more development of littoral environments) and changes in land use, with deforestation and farming causing an increase in runoff and sediment availability. This phenomenon has been documented in other Spanish karstic lakes: Estanya Lake (Morellón et al. 2008) in the Pre-Pyrenees, Taravilla Lake (Moreno et al. 2008) in the Iberian Range, and Zoñar Lake in Andalusia (Martín-Puertas et al. 2008). Floodplain aggradation in Iberian rivers from 910 to 500 cal yr BP (Benito et al. 2008) also supports an increase of agriculture and deforestation during medieval times.

The reduction of clastic input, higher primary productivity, and enhanced endogenic calcite precipitation in Montcortès Lake between 488 and 177 cal yr BP (1462–1773 AD) coincides with the onset and the first phases of the Little Ice Age (LIA), a humid and cold period in Europe (Pfister et al. 1998). In Spain, this period is characterized by higher river flood frequency between 520 and 265 cal yr BP (1430–1685 AD) (Thorndycraft and Benito 2006) and higher lake levels as documented in several sites, e.g. La Cruz Lake (Julià et al. 1998), Taravilla Lake (Moreno et al. 2008), Zoñar Lake (Martín-Puertas et al. 2008), Estanya Lake (Morellón et al. 2008). In one karstic lake (La Cruz), palynological studies have shown a relation between increasing farmlands (and a concomitant loss of forest areas), cooler temperatures and higher lake levels, with development of lacustrine varves (Julià et al. 1998). Nevertheless, the reduction of clastic input recognized in Montcortès Lake for this period may also be related to the economic and social crises during the fourteenth and fifteenth centuries causing significant depopulation of the area and abandonment of farmlands, crops and pastures (Rull et al. this volume).

The increase in turbidity current frequency in Montcortès during the nineteenth century coincides with the last phases of the LIA and the maximum expansion of agriculture and population in the Pyrenean Mountains (Morellón et al. this volume). During this pre-industrial period, traditional crop rotation was used to enhance cereal production and forest exploitation was the dominant practice in the mountains. In northeast Spain, documents indicate highest flood severity during AD 1840–1870 (Barriendos and Llasat 2003; Llasat et al. 2003). Thus, this period of increased clastic input during the nineteenth century would have been triggered by both climatic factors (more intense flooding during the last phases of the LIA) and anthropic activities.

The twentieth century increase in lake productivity may have been influenced by the increase in nutrients, due to more intensive use of the lake for tourism, and input of fertilizers and nutrient-rich wastes, i.e. cultural eutrophication. A similar case has been documented in Baldeggersee, Switzerland where the onset of lacustrine varve formation since 1885 AD was attributed to eutrophication (Fabian et al. 2003). The recent (since mid twentieth century) reduction of clastic input may be related to emigration from rural zones to urban, industrialized areas, which profoundly affected the Pallars region between 1960 and 1980 (Rull et al. this volume).

Conclusions

The changing nature of the finely laminated facies in the Montcortès Lake sediment sequence records the interplay between climate and human factors in the lake and the watershed for the last 6,000 cal years. Anoxic bottom conditions prevailed during this period and varves composed of triplets (calcite, organic, clastic laminae) or couplets (organic, clastic laminae), with some turbidite layers, were deposited in the deepest areas of the lake. Three major phases of gravitational processes occurred around 1,010, 1,600 and 6,000 cal yr BP.

Carbonate production and preservation coincided with periods of increased bioproductivity, and likely higher lake levels. Periods with no endogenic carbonate are related to periods of relatively lower lake level, high organic matter accumulation and less favourable conditions for calcite preservation (lower pH in the hypolimnion). According to the chronological model and detailed sedimentary facies analyses, relatively shallower lake levels with no carbonate production occurred during the period 6,000–3,800 cal yr BP, synchronous with the middle Holocene more arid period in the Iberian Peninsula. The transition to deeper lake conditions and the onset of carbonate production in the epilimnion started at 3,800 cal yr BP and continued until the present.

Periods of lower clastic input into the lake occurred during the Iberian-Roman Humid Period, the Little Ice Age (LIA) and the last 50 years. In contrast, periods of increased sediment delivery to the lake occurred during both drier (Medieval Climate Anomaly and the Middle Ages 690–1460 AD) and more humid (nineteenth century, end of LIA) periods, but always characterized by intense farming and higher human pressure in the watershed. Although perhaps modulated by climate and hydrological variability, changes in clastic input to the lake reflect modifications of agricultural practices and population pressure in the watershed.

Acknowledgments Financial support for this research was provided by the Spanish CICYT, through the projects LIMNOCLIBER (REN2003-09130-C02-02), IBERLIMNO (CGL2005-20236-E/CLI), LIMNOCAL (CGL2006-13327-C04-01) and GRACCIE (CSD2007-00067). Additional funding was provided by the Aragonese Regional Government–CAJA INMACULADA, which partially funded microfacies analysis at GFZ (Potsdam) through a travel grant. Juan Pablo Corella was supported by a PhD contract with CONAI+D (Aragonese Scientific Council for Research and Development), A. Moreno held a Ramón y Cajal programme post-doctoral contract, M. Rico a Juan de la Cierva contract from the Spanish Government and A. Pérez-Sanz a CONAI+D PhD fellowship. We are indebted to the GFZ and IPE-CSIC laboratory staffs for their collaboration in this research. We also thank Alberto Sáez and Clara Mangili for constructive criticisms of the earlier version of the manuscript.

References

Anderson R, Dean W (1988) Lacustrine varve formation trough time. Palaeogeogr Palaeoclimatol Palaeoecol 62:215–235

Bard E, Raisbeck G, Yiou F, Jouzel J (2000) Solar irradiance during the last 1200 yr based on cosmogenic nuclides. Tellus 52B:985–992

Bar-Matthews M, Ayalon A, Kaufman A, Wasserburg GJ (1999) The eastern Mediterranean paleoclimate as a reflection of regional events: Soreq cave, Israel. Earth Planet Sci Lett 166:85–95

Bar-Matthews M, Ayalon A, Gilmour MA, Matthews A, Hawkesworth CJ (2003) Sea-land oxygen isotopic relationships from planktonic foraminifera and speleothems in the Eastern Mediterranean region and their implication for paleorainfall during interglacial intervals. Geochim Cosmochim Acta 67:3181–3199

Barriendos M, Llasat MC (2003) The Case of the 'Maldá' Anomaly in the Western Mediterranean Basin (AD 1760–1800): an example of a strong climatic variability. Clim Chang 61:191–216

Benito G, Machado MJ, Pérez-González A (1996) Climate change and flood sensitivity in Spain. In: Branson J, Brown AG, Gregory KJ (eds) Global continental changes: the context of paleohydrology. The Geological Society of London, London, pp 85–98

Benito G, Thorndycraft VR, Rico M, Sánchez-Moya Y, Sopeña A (2008) Palaeoflood and floodplain records from Spain: evidence for long-term climate variability and environmental changes. Geomorphology 101:68–77

Blanco E, Casado M, Costa M, Escribano R, García Antón M, Génova M, Gómez A, Moreno J, Morla C, Regato P, Sainz Ollero H (1997) Los Bosques Ibéricos. Una Interpretación Geobotánica. Planeta, Barcelona, p 572

Bond G, Kromer B, Beer J, Muscheler R, Evans MN, Showers W, Hoffmann S, Lotti-Bond R, Hajdas I, Bonani G (2001) Persistent solar influence on north Atlantic climate during the Holocene. Science 294:2130–2136

Brauer A (2004) Annually laminated lake sediments and their palaeoclimatic relevance. In: Fischer H, Kumke T, Lohmann G, Flöser G, Miller H, von Storch H, Negendank JFW (eds) The climate in historical times. Towards a synthesis of Holocene proxy data and climate models. Springer, Berlin, pp 109–128

Camps J, Gonzalvo I, Güell J, López P, Tejero A, Toldrà X, Vallespinos F, Vicens M (1976) El lago de Montcortès, descripción de un ciclo anual. Oecología acuática 2: 99–100

Canals M, Got H, Julia R, Serra J (1990) Solution-collapse depressions and suspensates in the limnocrenic lake of Banyoles (NE Spain). Earth Surf Proc Land 15:243–254

Chung FH (1974a) Quantitative interpretation of X-ray diffraction patterns of mixtures: I. Matrix-flushing method for quantitative multicomponent analysis. J Appl Crystallogr 7:519–525

Chung FH (1974b) Quantitative interpretation of X-ray diffraction patterns of mixtures: II. Adiabatic principles of X-ray diffraction analysis of mixtures. J Appl Crystallogr 7:526–531

Cohen AS (2003) Paleolimnology. The history and evolution of lake systems. Oxford University Press, New York, p 500

Dean W (1999) The carbon cycle and biochemical dynamics in lake sediments. J Paleolimnol 21:375–393

Dragoni W (1998) Some consideration on climate changes, water resources and water needs in the Italian region south of 43°N. In: Issar AS, Brown N (eds) Water, environment and society in times of climate change. Kluwer Academic Publishers, Dordrecht, The Netherlands, pp 241–272

Drysdale R, Zanchetta G, Hellstrom J, Maas R, Fallick A, Pickett M, Cartwright I, Piccini L (2006) Late Holocene drought responsible for the collapse of Old World civilizations is recorded in an Italian cave flowstone. Geology 34:101–104

Fabian D, Zhou Z, Wehrli B, Friedl G (2003) Diagenetic cycling of arsenic in the sediments of eutrophic Baldeggersee, Switzerland. Appl Geochem 18:1497–1506

Giralt S, Moreno A, Valero-Garcés B, Sáez A, Bao R, Prego R, Pueyo JJ, González-Sampériz P, Taberner C (2008) A statistical approach to disentangle environmental forcings in a lacustrine record: the Lago Chungará case (Chilean Altiplano). J Paleolimnol 40:195–215

González-Sampériz P, Valero-Garcés BL, Moreno A, Morellon M, Navas A, Machin J, Delgado-Huertas A (2008) Vegetation changes and hydrological fluctuations in the Central Ebro Basin (NE Spain) since the Late Glacial period: saline lake records. Palaeogeogr Palaeoclimatol Palaeoecol 259:115–136

Julià R, Burjachs F, Dasí MJ, Mezquita F, Miracle RM, Roca JR, Seret G, Vicente E (1998) Meromixis origin and recent trophic evolution in the Spanish mountain lake La Cruz. Aquat Sci 60:279–299

Kelts K, Hsü KJ (1978) Freshwater carbonate sedimentation. In: Lerman A (ed) Lakes-chemistry, geology, physics. Springer, Berlin, pp 295–323

Kropelin S, Verschuren D, Lezine AM, Eggermont H, Cocquyt C, Francus P, Cazet JP, Fagot M, Rumes B, Russell JM, Darius F, Conley DJ, Schuster M, von Suchodoletz H, Engstrom DR (2008) Climate-driven ecosystem succession in the Sahara: the past 6000 years. Science 320: 765–768

Lamb H, Gasse F, Benkaddour A, El Hamoutl N, Van der Kaars S, Perkins WT, Pearce NJ, Roberts CN (1995)

Relation between century-scale Holocene arid intervals in tropical and temperate zones. Nature 373:134–137
Leira M (2005) Diatom responses to Holocene environmental changes in a small lake in northwest Spain. Quatern Int 140:90–102
Liu Z, Wang Y, Gallimore R, Notaro M, Prentice IC (2006) On the cause of abrupt vegetation collapse in North Africa during the Holocene: climate variability vs. vegetation feedback. Geophys Res Lett 33:L22709. doi:10.1029/2006GL028062
Llasat MC, Rigo T, Barriendos M (2003) The "Montserrat-2000" flash-flood event: a comparison with the floods that have occurred in the northeastern Iberian peninsula since the 14th century. Int J Climat 23:453–469
Macklin MG, Benito G, Gregory KJ, Johnstone E, Lewin J, Michczyñska DJ, Soja R, Starkel L, Thorndycraft VR (2006) Past hydrological events reflected in the Holocene fluvial record of Europe. Catena 66:145–154
Magny M (2006) Holocene fluctuations of lake levels in west-central Europe: methods of reconstruction, regional pattern, palaeoclimatic significance and forcing factors. In: Elias SA (ed) Encyclopedia of quaternary geology encyclopedia of quaternary science. Elsevier, Amsterdam
Mangili C, Brauer A, Plessen B, Moscariello A (2007) Centennial-scale oscillations in oxygen and carbon isotopes of endogenic calcite from a 15, 500 varve year record of the Piànico interglacial. Quaternary Sci Rev 26:1725–1735
Martín-Puertas C, Valero-Garcés BL, Mata P, González-Sampériz P, Bao R, Moreno A, Stefanova V (2008) Arid and humid phases in Southern Spain during the last 4000 Years: the Zoñar lake record, Córdoba. Holocene 18:907–921
Martín-Puertas C, Valero-Garcés BL, Brauer A, Mata MP, Delgado-Huertas A, Dulski P (2009) The Iberian-Roman Humid Period (2600–1600 cal yr BP) in the Zoñar Lake varve record (Andalucía, southern Spain). Quaternary Res 71:108–120
Meyers PA (2003) Applications of organic geochemistry to paleolimnological reconstructions: a summary of examples from the Laurentian Great Lakes. Org Geochem 34:261–289
Miracle MR, Vicente E, Pedrós-Alió C (1992) Biological studies of Spanish meromictic and stratified karstic lakes. Limnetica 8:59–77
Morellón M, Valero-Garcés B, Moreno A, González-Sampériz P, Mata P, Romero O, Maestro M, Navas A (2008) Holocene palaeohydrology and climate variability in northeastern Spain: The sedimentary record of Lake Estanya (Pre-Pyrenean range). Quatern Intern 181:15–31
Morellón M, Valero-Garcés BL, Vegas-Vilarrúbia T, González-Sampériz P, Romero Ó, Delgado-Huertas A, Mata P, Moreno A, Rico M, Corella JP (2009) Lateglacial and Holocene palaeohydrology in the western Mediterranean region: the Lake Estanya record (NE Spain). Quaternary Sci Rev (in press). doi: 10.1016/j.quascirev.2009.05.014
Moreno A, Valero-Garcés BL, González-Sampériz P, Rico M (2008) Flood response to rainfall variability during the last 2000 years inferred from the Taravilla Lake record (Central Iberian Range, Spain). J Paleolim 40:943–961
Noren AJ, Bierman PR, Steig EJ, Lini A, Southon J (2002) Millennial-scale storminess variability in the northeast United States during the Holocene epoch. Nature 419:821–824
Paillard D, Labeyrie L, Yiou P (1996) Macintosh program performs time-series analysis. Eos Trans 77:379
Pfister C, Luterbacher J, Schwarz-Zanetti G, Wegmann M (1998) Winter air temperature variations in Western Europe during the early and high middle ages (AD 750–1300). Holocene 8:535–552
Pla S, Catalan J (2005) Chrysophyte cysts from lake sediments reveal the submillennial winter/spring climate variability in the northwestern Mediterranean region throughout the Holocene. Climat Dynam 24:263–278
Reale O, Dirmeyer P (2000) Modeling the effects of vegetation on Mediterranean climate during the roman classical period part I: Climate history and model sensitivity. Global Planet Chang 25:163–184
Reimer PJ, Baillie MGL, Bard E, Bayliss A, Beck JW, Bertrand CJH, Blackwell PG, Buck CE, Burr GS, Cutler KB, Damon PE, Edwards RL, Fairbanks RG, Friedrich M, Guilderson TP, Hogg AG, Hughen KA, Kromer B, McCormac G, Manning S, Ramsey CB, Reimer RW, Remmele S, Southon JR, Stuiver M, Talamo S, Taylor FW, van der Plicht J, Weyhenmeyer CE (2004) IntCal04 terrestrial radiocarbon age calibration, 0 to 26 Cal Kyr BP. Radiocarbon 46:1029–1058
Rodríguez-Pascua MA, Becker A, Calvo JP, Davenport CA, Gómez-Gras D (2003) Sedimentart record of seismic events, with examples from recent and fossil lakes. In: Valero-Garcés B (ed) Limnogeology in Spain: a tribute to Kerry Kelts. Biblioteca de Ciencias. C.S.I.C, Madrid, pp 253–281
Romero-Viana L, Julià R, Camacho A, Vicente E, Miracle M (2008) Climate signal in varve thickness: Lake La Cruz (Spain), a case study. J Paleolim 40:703–714
Rosell J (1994) Mapa Geológico de España y Memoria. Escala 1:50.000, Hoja de Tremp (252). Instituto Tecnológico Geominero de España (IGME), Madrid
Sadori L, Giraudi C, Petitti P, Ramrath A (2004) Human impact at Lago di Mezzano (central Italy) during the Bronze Age: a multidisciplinary approach. Quatern Int 113:5–17
Schnurrenberger DW, Russell JM, Kelts K (2003) Classification of lacustrine sediments based on sedimentary components. J Paleolim 29:141–154
Seager R, Graham N, Herweijer C, Gordon AL, Kushnir Y, Cook E (2007) Blueprints for Medieval hydroclimate. Quaternary Sci Rev 26:2322–2336
Strasser M, Stegmann S, Bussmann F, Anselmetti FS, Rick B, Kopf A (2007) Quantifying subaqueous slope stability during seismic shaking: Lake Lucerne as model for ocean margins. Mar Geol 240:77–97
Thorndycraft VR, Benito G (2006) Late Holocene fluvial chronology of Spain: the role of climatic variability and human impact. Catena 66:34–41
Valero-Garcés BL, Navas A, Machín J, Stevenson T, Davis B (2000) Responses of a saline lake ecosystem in a semiaric region to irrigation and climate variability. Ambio 29:344–350
Valero-Garcés BL, González-Sampériz P, Navas A, Machín J, Mata P, Delgado-Huertas A, Bao R, Moreno A, Carrión JS, Schwalb A, González-Barrios A (2006) Human impact since Medieval times and recent ecological restoration in a Mediterranean lake: the laguna Zoñar (Spain). J Paleolim 35:441–465